

Evidence of X-ray plateaus driven by the magnetar spindown winds in gamma-ray burst afterglows

SHU-JIN HOU,^{1,2} SHUANG DU,^{3,2} TONG LIU,⁴ HUI-JUN MU,⁵ AND REN-XIN XU^{2,6}

¹*Department of Physics and Electronic Engineering, Nanyang Normal University, Nanyang, Henan 473061, China*
houshujingrb@163.com

²*State Key Laboratory of Nuclear Physics and Technology, School of Physics, Peking University, Beijing 100871, China*
r.x.xu@pku.edu.cn

³*College of Mathematics and Physics, Wenzhou University, Wenzhou, Zhejiang 325035, China*
dushuang@pku.edu.cn

⁴*Department of Astronomy, Xiamen University, Xiamen, Fujian 361005, China*
tongliu@xmu.edu.cn

⁵*International Laboratory for Quantum Functional Materials of Henan and School of Physics and Microelectronics, Zhengzhou University, Zhengzhou, Henan 450001, China*

⁶*Kaoli Institute for Astronomy and Astrophysics, Peking University, Beijing 100871, China*

ABSTRACT

The central engine of gamma-ray bursts (GRBs) remains an open and forefront topic in the era of multimessenger astrophysics. The X-ray plateaus appear in some GRB afterglows, which are widely considered to originate from the spindown of magnetars. According to the stable magnetar scenario of GRBs, an X-ray plateau and a decay phase as $\sim t^{-2}$ should appear in X-ray afterglows. Meanwhile, the “normal” X-ray afterglow is produced by the external shock from GRB fireball. We analyze the Neil Gehrels *Swift* GRB data, then find three gold samples, which have an X-ray plateau and a decay phase as $\sim t^{-2}$ superimposed on the jet-driven normal component. Based on these features of the lightcurves, we argue that the magnetars should be the central engines of these three GRBs. Future joint multimessenger observations might further test this possibility, then which can be beneficial to constrain GRB physics.

Keywords: gamma-ray burst: general - gamma-ray burst: individual (GRBs 060413, 060607A, 061202, and 191122A) - stars: magnetars

1. INTRODUCTION

The central engine of gamma-ray bursts (GRBs) remains a mystery. The millisecond magnetars (e.g., Usov 1992; Duncan & Thompson 1992; Dai & Lu 1998a,b; Zhang & Mészáros 2001; Bucciantini et al. 2007; Metzger et al. 2011; Du 2020) and black hole (BH) hyperaccretion (e.g., Popham et al. 1999; Narayan et al. 2001; Kohri et al. 2005; Gu et al. 2006; Liu et al. 2007; Kawanaka et al. 2013; Hou et al. 2014) are two main candidates of GRB central engines. For the recent reviews see Liu et al. (2017) and Zhang (2018). GRB prompt emission is generated by the internal shock in the ultra-relativistic jets, and the following afterglow is produced by the external shock (Rees & Mészáros 1994; Sari et al. 1998). The lightcurves of prompt emission are usually irregular, but the afterglows generally have five components (e.g., Zhang et al. 2006).

The plateaus (shallow decays) are often seen in X-ray afterglow, which are usually thought to be caused

by energy injected into the jets. The energy may be extracted from rotating magnetars or fallback accretions (e.g., Dai & Lu 1998a; Zhang & Mészáros 2001; Liu et al. 2017; Du et al. 2019; Huang & Liu 2021). Meanwhile, the superimposed normal decay is dissipated through the interaction between the jet and circumburst medium (e.g., Sari et al. 1998). Their typical decay index is predicted to be ~ 1.2 , but the observations are in the range of $0 - 1.5$ under the different circumstances and conditions (e.g., Sari et al. 1998; Zhang et al. 2006). However, the spindown winds might not be injected into GRB jets, but dissipated behind GRB jets to power X-ray plateaus in the GRB magnetar model (Du 2020). In this scenario, the indices of the decays after plateaus are ≥ 2 (Zhang & Mészáros 2001).

The magnetar could be born in the center of a massive collapsar or a neutron star (NS) binary merger (e.g., Giacomazzo et al. 2011; Faber & Rasio 2012; Liu et al. 2021). For the hypermassive magnetar, the very short life leads that the spindown winds can not accu-

accumulate enough energy to produce observable features (Rosswog et al. 2000). For the supramassive magnetar case, as discussed in Du (2020), it (with life time $\gtrsim 100$ s) has enough time to power the energetic spindown winds to generate the X-ray plateau followed by a steeper decay (with decay index > 3). This phenomenon is called internal X-ray plateaus, which is understood as the collapse of a supramassive magnetar into a BH after the magnetar spindown (e.g., Troja et al. 2007; Rowlinson et al. 2010; Chen et al. 2017; Hou et al. 2018). In the stable magnetar case, the index of the decay following plateau is ~ 2 (Zhang & Mészáros 2001). It is interesting that the X-ray transient CDF-S XT2 with an X-ray plateau and a decay component as $\sim t^{-2}$ is well explained by the model of magnetar spindown winds under the stable magnetar scenario (Xue et al. 2019).

We consider that the types of the GRB central engines can be judged by the similar observational features. Focus on the model of magnetar spindown winds, we propose the following criteria. First, there should exist an X-ray plateau and a decay component as $\sim t^{-2}$ in X-ray afterglows. However, this rule is not enough to prove a magnetar in the center of GRBs, because X-ray plateaus can be explained by involving the off-axis or precessing jets (e.g., Beniamini et al. 2020; Oganessian et al. 2020; Huang & Liu 2021) and the classical energy injections (e.g., Dai & Lu 1998a; Zhang & Mészáros 2001). Second, an additional X-ray radiation with decay index ~ 1.2 originating in the external shock should be superimposed with the plateau and a decay phase (e.g., Sari et al. 1998; Zhang et al. 2006). This additional component indicates an X-ray plateau with a decay phase as $\sim t^{-2}$ is not produced by the external shock but the magnetar itself.

By using the above rules on the observations, the coincident sources could be satisfied with the model of magnetar spindown winds and further verify the existence of magnetars. The remaining part of this paper is organized as follows. We present our model in Section 2. The study of three cases is shown in Section 3. Section 4 is the conclusions and a brief discussion.

2. SUPERPOSITIONS BETWEEN GRB JETS AND MAGNETAR SPINDOWN WINDS

For a GRB originated from a stable magnetar, as proposed in Du (2020), its X-ray afterglow should be composed by the X-ray radiation from the winds driven by the magnetar spindown and magnetar-driven jets.

The evolution of the spindown luminosity of a magnetar can be expressed as

$$L_{\text{SD}} = \frac{8\pi^4 B_{\text{eff}}^2 R_*^6}{3c^3 P^4}, \quad (1)$$

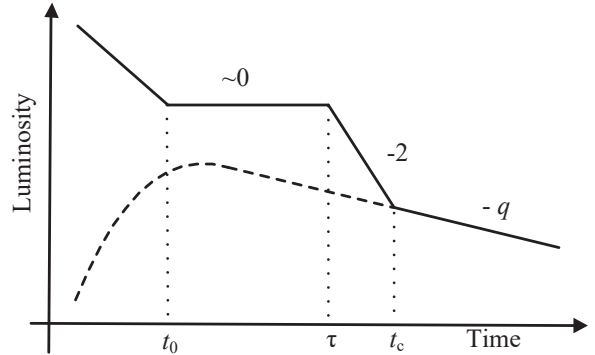


Figure 1. Schematic diagram of X-ray lightcurve contributed by magnetar spindown winds and GRB jets. There is a “tail” of prompt emission before t_0 , and the X-ray emission turns to be dominated by the spindown wind emission until $t > t_c$. After t_c , the X-ray emission is dominated by GRB jets. According to the standard external shock model, the typical value of q is ~ 1.2 .

where B_{eff} is the effective magnetic field strength on the NS surface (includes all the contribution that deviates from the dipole magnetic field), R_* is the equatorial radius, and P is the NS period (Zhang & Mészáros 2001).

If we consider that B_{eff} is a constant, the evolution of the X-ray luminosity L_{W} produced by the spindown winds is

$$L_{\text{W}} = L_{\text{W},0} \left(1 + \frac{t}{\tau}\right)^{-2}, \quad (2)$$

and the characteristic spindown time scale τ is

$$\tau = \frac{3c^3 I P_0^2}{4\pi^2 B_{\text{eff}}^2 R_*^6}, \quad (3)$$

where $L_{\text{W},0} = \eta L_{\text{SD},0}$ is the initial X-ray luminosity of the spindown wind, η is the efficiency of magnetic energy converting into X-ray emission, $L_{\text{SD},0}$ is the initial spindown luminosity, I and P_0 are rotational inertia and initial period of the magnetar, and t is the time from the burst, respectively. There is an X-ray plateau at $t < \tau$. When t is much greater than τ , there is a decay component as $\sim t^{-2}$.

The luminosity of the X-ray emission from the jets, which is called the external shock model, can be empirically given by

$$L_{\text{J}} = L_{\text{J},0} t^{-q}, \quad (4)$$

where $L_{\text{J},0}$ is the X-ray luminosity of the jets and q is the decay index with the typical value ~ 1.2 as shown in Figure 1.

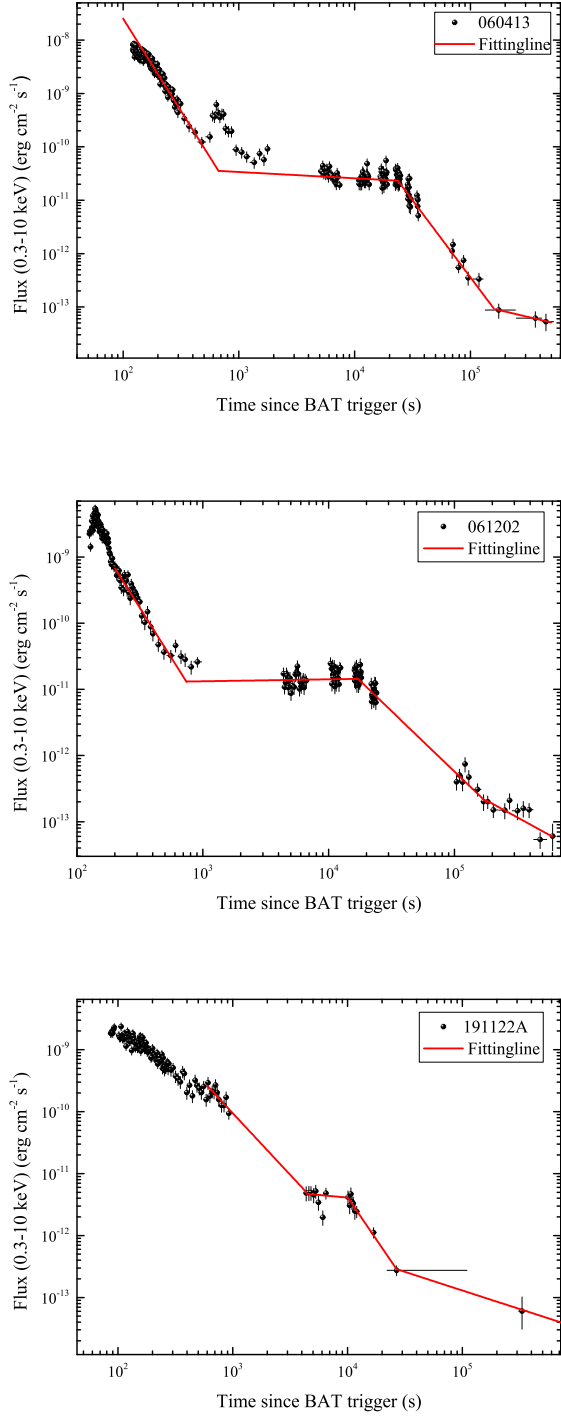


Figure 2. X-ray lightcurves of GRBs 060413, 061202, and 191122A in 0.3–10 keV band. Red lines denote the best fitting lines with the multi-powerlaw function.

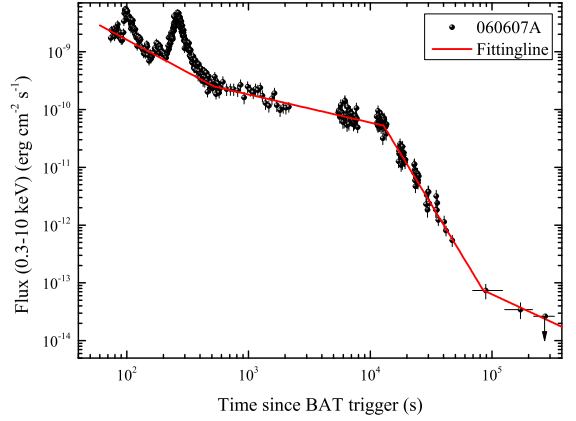


Figure 3. X-ray lightcurves of GRB 060607A in 0.3–10 keV band. The slope after the plateau is 3.48. In this case, an NS may collapse into a BH at the later stage.

Since the decay of the X-ray emission from GRB jets is slower than that from spindown winds after τ by comparison between Equations (2) and (4), there is a situation that L_W is always smaller than L_J . There is also the possibility of another situation that the whole afterglow is dominated by the spindown winds. In those situations, the components from non-dominant contributions are hardly identified through the lightcurve. We are not interested in those situations and will not discuss here.

It is worth discussing the situation that the X-ray emission is alternately dominated by the spindown winds and GRB jets. In early stage of the X-ray afterglow, the “tail” of prompt emission and the emission from spindown winds may be very strong, so the X-ray emission from GRB jets may be masked. Here we only discuss that the early phases of X-ray afterglows are dominated by spindown winds and the later phases are dominated by GRB jets.

Based on the relation of $L_W = L_J$, we can obtain the solutions as

$$\begin{cases} t_c = \left(\frac{L_{W,0}}{L_{J,0}}\right)^{\frac{1}{-q}} & \text{if } t \ll \tau \\ t_c = \left(\tau^2 \frac{L_{W,0}}{L_{J,0}}\right)^{\frac{1}{2-q}} & \text{if } t \gg \tau \end{cases} \quad (5)$$

Therefore, if there is a “tail” of prompt emission before t_0 , the first solution t_c is not visible in the lightcurve, then the X-ray emission turns to be dominated by the spindown wind emission until $t > t_c$. After t_c , the X-ray emission is dominated by the jets. The corresponding lightcurve of three typical example is shown in Figure 1.

It needs to be emphasized that the X-ray plateaus can be explained by the off-axis or precessing jets with whatever type of central engines. However, these models

Table 1. Fitting results of X-ray lightcurves with multi-powerlaw functions.

GRBs	α_1 (err)	α_2 (err)	α_3 (err)	α_4 (err)
060413	3.46 (0.13)	0.12 (0.05)	2.89 (0.14)	0.52 (0.04)
061202	3.02 (0.17)	-0.03 (0.06)	1.83 (0.05)	1.04 (0.29)
191122A	1.99 (0.12)	0.17 (0.22)	2.72 (0.14)	0.60
060607A	1.13 (0.04)	0.49 (0.02)	3.48 (0.11)	0.98 (0.18)

Notes:

(1) α_1 denotes the slope of the steep decay component (the “tail” of prompt emission); α_2 and α_3 represent the slopes of the plateau and the following decay component, respectively; and α_4 corresponds the decay index of the component at later stage.

(2) Due to a lack of late-time date, α_4 is fixed for GRB 191122A. α_3 for GRB 060607A is ~ 3.48 , which indicates a collapsing NS progenitor and is not suitable for our sample.

cannot explain the decay index changes at later stage of X-ray afterglows. The inflexion means that there are two different components, which is predicted by the model of the magnetar spindown winds. The X-ray plateaus with the following decay segments as $\sim t^{-2}$ is powered by a magnetar spindown winds. The X-ray afterglows following the spindown wind segment is from the standard external shock of the jets.

3. SAMPLES

According to the model discussed above, we select candidates according to the following criteria: (i) a plateau should exist in the X-ray emission lightcurve; (ii) after the plateau, there is a steeper decay with index ~ 2 ; (iii) at the later stage of the X-ray lightcurve, there is another decay component with index ~ 1.2 . This component is the key criteria of our sample.

According to the above criteria, we found three gold samples in the Neil Gehrels *Swift* GRB data, i.e., GRBs 060413, 061202, and 191122A. All of them belong to the long-duration GRBs. The data are from the UK *Swift* Science Data Center at the University of Leicester (Evans et al. 2007, 2009). The afterglows of these bursts all contain multiple components. There are significant flares in GRBs 060413 and 061202. At late times, the decay index of afterglow can be constrained even though the data are sparse.

We employ the multiple broken power-law functions to fit their X-ray lightcurves. The fitting results of four indices α_1 , α_2 , α_3 , and α_4 are listed in Table 1. The plateau component are all flat with the decay indices less than ~ 0.2 . After the plateau, their decay indices are 2.89, 1.83, and 2.72, respectively. These values are basically consistent with the slope of the magnetar spindown process. The indices of the last components are 0.52, 1.04, and 0.60, respectively. Under the different circumstances and conditions, the slope range of the lightcurve from the external shock model could be 0–1.5 (e.g., Sari et al. 1998; Zhang et al. 2006), so

we reasonably believe that these components come from GRB jets and further the central engines of these three GRBs should be magnetars.

In our samples, only the redshift of GRB 061202 is measured, i.e., $z = 2.25$. The X-ray luminosity of plateau L_W can be expressed as

$$L_W = \frac{4\pi D_L^2 F_W}{1+z}, \quad (6)$$

where D_L is the luminosity distance and F_W is the flux of plateau. By fitting, we get that F_W and τ are $\sim 1.0 \times 10^{-11}$ erg s $^{-1}$ cm $^{-2}$ and $\sim 1.8 \times 10^4$ s, respectively. Then L_W can be estimated to be $\sim 4.0 \times 10^{48}$ erg s $^{-1}$. Assuming that the rotational inertia of the magnetar is 10^{45} g cm 2 and the radius of NS is 10 km (e.g., Li et al. 2020), we can obtain that the isotropic energy of plateau $E_P \sim F_W \tau \simeq 2.4 \times 10^{52}$ ergs. According to Equations (1) and (3), the effective magnetic field strength on the NS surface B_{eff} and initial period P_0 are calculated, $\sim 5.0 \times 10^{14}$ G and ~ 1.1 ms, respectively. These values are satisfied with the magnetar model.

4. CONCLUSIONS AND DISCUSSION

In this paper, we analyze the shapes of lightcurves produced by magnetars spindown winds, which have an X-ray plateau and a decay component as $\sim t^{-2}$. According to the fireball model of GRBs, the X-ray afterglow is produced by the external shock from jets at the same time. However, the “tail” of prompt emission and the emission from spindown winds may be powerful at the early stage of X-ray afterglow, so the X-ray emission from the jets may be masked. We only discussed that the early phases of X-ray afterglow are dominated by the spindown winds and the later phases are dominated by jets. So there is a state transition in the lightcurve, which is a change in slope at the later stage of afterglows. We emphasize that the presence of the jet component is very important, because it supports the idea that the X-ray plateau arises from a component with a

different origin. By systematically analyzing the XRT lightcurves of GRBs detected by the Neil Gehrels *Swift* observatory, we find three gold samples to be consistent with the model of the magnetar spindown winds. Taking GRB 061202 as an example, the E_P , B_{eff} , and P_0 are estimated. They are all within the ranges of typical magnetar parameters. Since the features of the detectable MeV neutrinos and gravitational waves from (newborn) magnetars and BH hyperaccretion are distinguishable (e.g., Liu et al. 2016; Wei et al. 2019; Wei & Liu 2020), future joint multimessenger observations might provide more evidences on the magnetar-driven GRBs.

The above discussion is based on a stable magnetar. If the magnetar is a supramassive one, the corresponding X-ray lightcurve is similar to that in Figure 1, but the spindown time τ should be changed to the break time t_B (corresponding to the collapse time of the magnetar), and the slope of the segment following the plateau should be steeper (with decay index > 3). For example, the decay index following the plateau is 3.48 in GRB 060607A as shown in Figure 3. In some GRBs, the slopes even go up to ~ 9 (e.g., Troja et al. 2007). The internal X-ray plateaus is thought to go through a spindown

process and then collapse into a BH (e.g., Troja et al. 2007; Chen et al. 2017; Hou et al. 2018).

A magnetar might be the central engine of X-ray transient CDF-S XT2 (e.g., Xue et al. 2019; Xiao et al. 2019), this process only explains the spindown wind of the magnetar and could not see the slow decay which is powered by external shock. In our scenario, we consider that the components including the contributions of the jets and the magnetar spindown winds are the more reliable evidence for the existence of magnetars.

ACKNOWLEDGEMENT

We acknowledge the use of the public data from the Neil Gehrels *Swift* data archive and the UK *Swift* Science Data Center at the University of Leicester. This work is supported by the National Natural Science Foundation of China under grants U1938116, 11822304, 12173031, and 12103047, the National Key R&D Program of China No. 2017YFA0402602, the National SKA Program of China No. 2020SKA0120100, the Natural Science Foundation of Henan Province of China under grant 212300410290, and China Postdoctoral Science Foundation under grant 2019TQ0288.

REFERENCES

- Beniamini, P., Duque, R., Daigne, F., et al. 2020, MNRAS, 492, 2847
- Bucciantini, N., Quataert, E., Arons, J., et al. 2007, MNRAS, 380, 1541
- Chen, W., Xie, W., Lei, W.-H., et al. 2017, ApJ, 849, 119
- Dai, Z. G. & Lu, T. 1998a, A&A, 333, L87
- Dai, Z. G. & Lu, T. 1998b, PhRvL, 81, 4301
- Du, S. 2020, ApJ, 901, 75
- Du, S., Zhou, E., & Xu, R. 2019, ApJ, 886, 87
- Duncan, R. C. & Thompson C. 1992, ApJ, 392, L9
- Evans, P. A., Beardmore, A. P., Page, K. L., et al. 2007, A&A, 469, 379
- Evans, P. A., Beardmore, A. P., Page, K. L., et al. 2009, MNRAS, 397, 1177
- Faber, J. A. & Rasio, F. A. 2012, Living Reviews in Relativity, 15, 8
- Giacomazzo, B., Rezzolla, L., & Baiotti, L. 2011, PhRvD, 83, 044014
- Gu, W.-M., Liu, T., & Lu, J.-F. 2006, ApJL, 643, L87
- Hou, S.-J., Liu, T., Gu, W.-M., et al. 2014, ApJL, 781, L19
- Hou, S.-J., Liu, T., Xu, R.-X., et al. 2018, ApJ, 854, 104
- Huang, B.-Q. & Liu, T. 2021, ApJ, 916, 71
- Kawanaka, N., Piran, T., & Krolik, J. H. 2013, ApJ, 766, 31
- Kohri, K., Narayan, R., & Piran, T. 2005, ApJ, 629, 341
- Li, A., Zhu, Z.-Y., Zhou, E.-P., et al. 2020, Journal of High Energy Astrophysics, 28, 19
- Liu, T., Gu, W.-M., Xue, L., et al. 2007, ApJ, 661, 1025
- Liu, T., Gu, W.-M., & Zhang, B. 2017, NewAR, 79, 1
- Liu, T., Wei, Y.-F., Xue, L., et al. 2021, ApJ, 908, 106
- Liu, T., Zhang, B., Li, Y., et al. 2016, PhRvD, 93, 123004
- Metzger, B. D., Giannios, D., Thompson, T. A., et al. 2011, MNRAS, 413, 2031
- Narayan, R., Piran, T., & Kumar, P. 2001, ApJ, 557, 949
- Oganesyan, G., Ascenzi, S., Branchesi, M., et al. 2020, ApJ, 893, 88
- Popham, R., Woosley, S. E., & Fryer, C. 1999, ApJ, 518, 356
- Rees, M. J. & Mészáros, P. 1994, ApJL, 430, L93
- Rosswog, S., Davies, M. B., Thielemann, F.-K., et al. 2000, A&A, 360, 171
- Rowlinson, A., O'Brien, P. T., Tanvir, N. R., et al. 2010, MNRAS, 409, 531
- Sari, R., Piran, T., & Narayan, R. 1998, ApJL, 497, L17
- Troja, E., Cusumano, G., O'Brien, P. T., et al. 2007, ApJ, 665, 599
- Usov, V. V. 1992, Nature, 357, 472
- Wei, Y.-F. & Liu, T. 2020, ApJ, 889, 73
- Wei, Y.-F., Liu, T., & Song, C.-Y. 2019, ApJ, 878, 142
- Xiao, D., Zhang, B.-B., & Dai, Z.-G. 2019, ApJL, 879, L7

Xue, Y. Q., Zheng, X. C., Li, Y., et al. 2019, *Nature*, 568,
198

Zhang, B. 2018, *The Physics of Gamma-Ray Bursts*
(Cambridge: Cambridge Univ. Press)

Zhang, B., Fan, Y. Z., Dyks, J., et al. 2006, *ApJ*, 642, 354

Zhang, B. & Mészáros, P. 2001, *ApJL*, 552, L35